



Article

Identification of In Vitro Metabolites of Synthetic Phenolic Antioxidants BHT, BHA, and TBHQ by LC-HRMS/MS

Ons Ousji and Lekha Sleno *

Chemistry Department, Université du Québec à Montréal, Downtown Station, P.O. Box 8888, Montréal, QC H3C 3P8, Canada; ons.ousji@gmail.com

* Correspondence: sleno.lekha@uqam.ca

Received: 30 October 2020; Accepted: 11 December 2020; Published: 15 December 2020



Abstract: Butylated hydroxytoluene (BHT) and its analogs, butylated hydroxyanisole (BHA) and tert-butyl-hydroquinone (TBHQ), are widely used synthetic preservatives to inhibit lipid oxidation in the food, cosmetic and pharmaceutical industries. Despite their widespread use, little is known about their human exposure and related biotransformation products. The metabolism of these compounds was investigated using in vitro incubations with human and rat liver fractions. Liquid chromatography coupled to high-resolution tandem mass spectrometry was employed to detect and characterize stable and reactive species formed via oxidative metabolism, as well as phase II conjugates. Several oxidative metabolites have been detected, as well as glutathione, glucuronide, and sulfate conjugates, many of which were not previously reported. A combination of accurate mass measurements, MS/MS fragmentation behavior, and isotope-labeling studies were used to elucidate metabolite structures.

Keywords: BHT; BHA; synthetic antioxidant; metabolites; in vitro incubations; liquid chromatography; high-resolution tandem mass spectrometry

1. Introduction

Synthetic phenolic antioxidants were developed in the late 1940s [1]. They have been used in food, pharmaceuticals, cosmetic, and petrochemical industries to increase shelf life and to improve the quality, freshness, taste, and texture of consumer products [2]. They are widely used to trap free radicals and delay lipid oxidation in various products [1]. Despite their widespread use, very little is known about human exposure or environmental emissions, which has led to public concern about their health effects and environmental contamination [3]. Butylated hydroxytoluene (BHT), butylated hydroxyanisole (BHA), and tert-butyl-hydroquinone (TBHQ) are among the most used synthetic phenolic antioxidants [4].

BHT, the most frequently used synthetic phenolic antioxidant, is added to food, pharmaceuticals, and cosmetics, as well as an additive in rubber, plastics, mineral oil, and printing inks [5,6]. Reports on BHT toxicity and side effects have been somewhat contradictory. Some studies have shown positive effects of BHT, such as enhancing the intracellular levels of glutathione and related enzymes in rat [7], protecting against cancer due to its antioxidant activity [8], and having tumor reducing effects [6]. On the other hand, it has been shown to cause renal and hepatic damage in rats, increase liver weight, decrease the activities of several hepatic enzymes and exhibit toxic effects in lung tissue [6]. BHT toxicity has been mainly attributed to its metabolism. For instance, Nagai et al. reported that BHT-quinone, one of the major metabolites of BHT, cleaves DNA strands [9]. Moreover, Kupfer et al. [10] demonstrated lung toxicity and tumor production caused by hydroxylated metabolites of BHT.

BHA, a close analog of BHT, is usually found as an isomeric mixture, containing the major 3-*tert*-butyl-4-hydroxyanisole (3-BHA) (90%) and the minor 2-*tert*-butyl-4-hydroxyanisole (2-BHA) (10%) [11]. It has been used as a food additive since the late 1950s [12]. It is also used in animal feed, cosmetics, pharmaceuticals, rubber, biodiesel, and petroleum products [13]. Some studies on BHA have revealed beneficial effects, with anti-tumor and nephroprotective potential [14,15]. Nevertheless, BHA has been shown to be an endocrine disrupter and a carcinogen in rats [16,17]. It can also perturb adipogenesis and increase the incidence of obesity [11,17]. The effects of BHT and BHA on various organs (liver, lung, kidney, blood system, and reproductive system) have been reviewed [18].

TBHQ is also added to a wide range of foods, such as unsaturated vegetable oils, residual frying oils, lard, and infant formula, as well as in biodiesel [19,20]. Several studies documented the chemoprotective effects of TBHQ. However, other *in vitro* studies, indicated that it can cause DNA damage and *in vivo* tests suggest it may be carcinogenic, cytotoxic, and genotoxic [19,21]. TBHQ is a major metabolite of BHA resulting from a demethylation reaction [22], and it has been suggested to contribute to the carcinogenicity of BHA [19].

Despite the large number of scientific papers describing the controversial effects of BHT and its analogs using *in vitro* and *in vivo* animal models, only very few studies have described these synthetic antioxidants in humans [1,5,23,24]. BHT and BHA have been banned in Japan since 1958 and have use restrictions in infant formulas in the UK. [25] However, BHT, BHA, and TBHQ are currently allowed in Canada, United States, Korea, and certain countries within the European Union [1,3,26,27]. They are categorized as “generally recognized as safe” (GRAS) by the U.S. Food and Drug Administration (FDA) and safe to use in cosmetics by the Cosmetic Ingredient Review (CIR) Expert Panel [1,2,6,26], while the International Agency for Research on Cancer (IARC) classifies BHT as non-carcinogenic (based on limited evidence), BHA as reasonably anticipated to be a human carcinogen and TBHQ as not carcinogenic [13,16,27].

The metabolism of BHT and analogs has been studied by gas chromatography coupled to mass spectrometry (GC-MS) [1,24,28], and by high-performance liquid chromatography (HPLC) [6]. The tissue distribution, excretion, and metabolism of BHT in mice were recently investigated using HPLC-MS/MS and GC-MS [29].

The potential for human exposure of BHT and its analogs, as well as the lack of information surrounding this exposure, support the need to study their biotransformation reactions, especially concerning the formation of reactive metabolites.

In this study, the metabolism of BHT, BHA, and TBHQ was evaluated using liver microsomes and subcellular (S9) fractions from humans and rats. Oxidative metabolites, glutathione (GSH) adducts, glucuronides, and sulfate conjugates have been characterized by liquid chromatography coupled to a quadrupole-time-of-flight high-resolution tandem mass spectrometer. Isotope-labeled BHT analogs were employed to aid in the structural elucidation of metabolites. Two metabolites of BHT, DBP, and BHT-acid, were also purchased to confirm their presence in BHT incubations. The metabolism of these two compounds was also studied to confirm metabolic pathways.

2. Results and Discussion

2.1. Metabolism of BHT

For the purpose of studying the various metabolic routes of BHT, an LC-MS/MS method was optimized. A biphenyl solid-core column using 5 mM ammonium acetate and acetonitrile as mobile phases A and B, respectively, yielded significant signal increase over using formic acid as an additive, as well as ameliorating peak shapes for many of the metabolites found in this study. BHT eluted with a retention time of 14.3 min with our optimized gradient (Table 1). The high-resolution MS/MS spectrum of deprotonated BHT (m/z 219.1760) with a collision energy of 30 V, presented in Figure 1, exhibits only one major fragment ion at m/z 203.1429 ($C_{14}H_{19}O^-$), via the loss of CH_4 . Otherwise, this molecule is

quite resistant to fragmentation, and when collision energy was increased to form other structurally characteristic fragments, most of the signal was lost and no clear product ions were observed.

Table 1. Summary of MS/MS data for BHT and metabolites in negative ion mode.

Metabolite	Formula	m/z [M-H] ⁻	ppm	RT (min)	Selected MS/MS Fragments *
BHT	C ₁₅ H ₂₄ O	219.1760	2.7	14.3	203.1439
BHT + O (1)	C ₁₅ H ₂₄ O ₂	235.1708	2.1	13.4	217.1598, 160.0895, 145.0657
BHT + O (2)	C ₁₅ H ₂₄ O ₂	235.1705	0.8	14.1	217.1597, 205.1597 233.1547, 221.1557, 203.1444, 160.0893, 146.0746
BHT + 2O	C ₁₅ H ₂₄ O ₃	251.1660	2.9	11.9	217.1234
BHT-aldehyde	C ₁₅ H ₂₂ O ₂	233.1552	2.2	14.0	205.1592
BHT-acid	C ₁₅ H ₂₂ O ₃	249.1501	2.2	9.8	231.1400, 219.1399
BHT-aldehyde + O	C ₁₅ H ₂₂ O ₃	249.1503	3.0	13.5	189.1289
DBP	C ₁₄ H ₂₂ O	205.1600	1.2	14.2	164.0848, 149.0601
BHQ	C ₁₄ H ₂₂ O ₂	221.1549	0.9	8.3	306.0772, 272.0892, 254.0788, 160.0078, 143.0463, 128.0353 306.0758, 288.0646, 272.0882, 254.0778, 160.0078, 143.0465, 128.0348
BHT-2H + GSH	C ₂₅ H ₃₉ N ₃ O ₇ S	524.2436	0.1	8.5	492.2179, 272.0886, 254.0793, 237.1316, 143.0462, 128.0353
BHT + O-2H + GSH	C ₂₅ H ₃₉ N ₃ O ₈ S	540.2381	-0.7	7.6	205.1595, 175.0247, 113.0240, 85.0291 193.0360, 131.0341, 113.0244, 85.0289 249.1491, 193.0354, 175.0247, 131.0344, 113.0239, 72.9929
DBP-2H + GSH	C ₂₄ H ₃₇ N ₃ O ₇ S	510.2287	1.5	8.2	221.1537, 175.0135, 113.0242, 85.0290
DBP + gluc	C ₂₀ H ₃₀ O ₇	381.1924	1.4	8.7	221.1539, 164.0844, 80.9645, 79.9576
BHT + O + gluc	C ₂₁ H ₃₂ O ₈	411.2026	0.5	8.8	
BHT-acid + gluc	C ₂₁ H ₃₀ O ₉	425.1820	0.9	8.3	
BHQ + gluc	C ₂₀ H ₃₀ O ₈	397.1864	-1.0	7.1	
BHQ + SO ₃	C ₁₄ H ₂₂ O ₅ S	301.1117	0.8	9.0	

* fragment ions of >20% intensity relative to base peak are listed here in bold, base peak in each spectrum is underlined.

Both human and rat microsomes yielded similar metabolic profiles for all tested compounds and incubations conditions. Throughout the manuscript, representative chromatograms from the human incubations are shown. All metabolites were confirmed with accurate mass measurements within 5 ppm of the theoretical exact masses. When BHT was incubated under oxidative conditions, several metabolites were detected, as shown in Figure 2. Two hydroxylated BHT metabolites (BHT + O) were detected, eluting at 13.4 and 14.1 min (Table 1). The comparison of their HRMS/MS spectra showed a common water loss at m/z 217.159 confirming that, in both cases, the oxygen is not added to the aromatic ring. To investigate whether the oxygen is added to the *para*-methyl or on a *t*-butyl group, isotope-labeled BHTs were also incubated (Table 2). Using BHT-d₃ and BHT-d₂₀, the BHT + O peak at 13.4 min, was shifted from m/z 235.1708 to 237.1834 and 255.2967, respectively (Table 2), indicating that the oxidation occurs on the methyl group. While for the isomer at 14.1 min, it was shifted from m/z 235.1705 to 238.1893 and 254.2903, respectively (Table 2), proving that the oxidation occurs on a *t*-butyl group. Di-hydroxylated BHT was also detected at 11.9 min (Figure 2) with m/z 251.1660 (C₁₅H₂₃O₃⁻, 2.9 ppm), and its MS/MS spectrum showed two water losses (Table 1). Both BHT-d₃ and BHT-d₂₀ analogs lost one deuterium atom, therefore one oxygen is added on the methyl group and the second one is on the *t*-butyl, in accordance with the two BHT + O isomers mentioned above. BHT-aldehyde via the oxidation of the *p*-methyl group was also detected at 14.0 min (Table 1) [6], confirmed by the fact that BHT-d₃ lost all three labels during this metabolic transformation, while BHT-d₂₀ did not lose any.

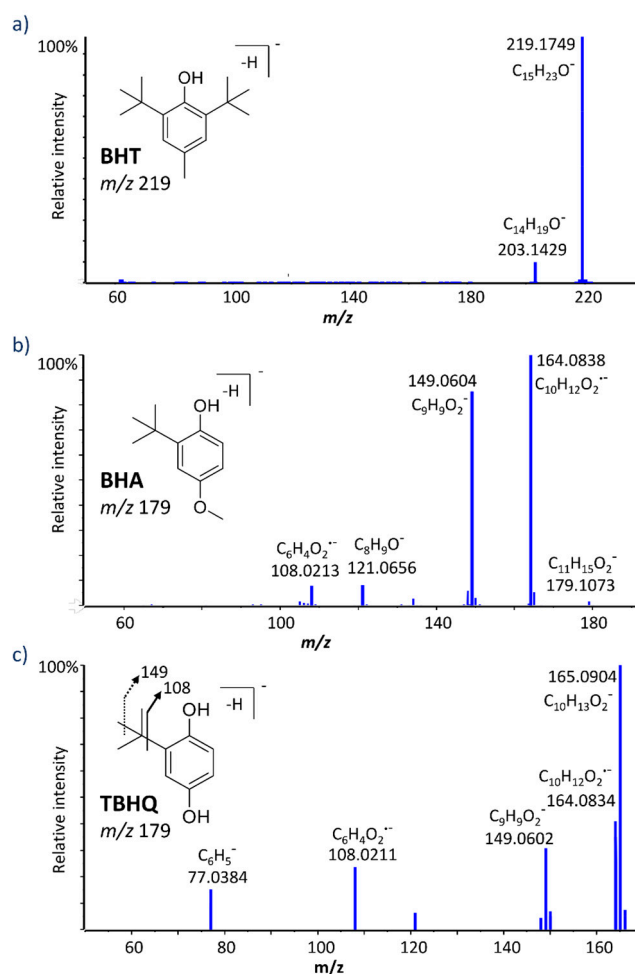


Figure 1. High resolution MS/MS spectra for deprotonated butylated hydroxytoluene (BHT) (a), butylated hydroxyanisole (BHA) (b), and tert-butyl-hydroquinone (TBHQ) (c).

Another two oxidative metabolites were detected at 9.8 and 13.5 min, both corresponding to $C_{15}H_{21}O_3^-$ (m/z 249.150). The isomer eluting at 9.8 min showed a characteristic fragment at m/z 205.1592 corresponding to the loss of CO_2 (Table 1), and lost the three labels from BHT- d_3 (Table 2), proving it to be BHT-acid, where the methyl group is oxidized to a carboxylic acid. To further confirm this, the commercial standard of BHT-acid was purchased and showed the same retention time (Figure S1) and MS/MS fragmentation behavior. The second isomer (Table 1), at 13.5 min, presented a water loss consistent with an oxidation on a methyl group, as well as the loss of CH_2O . The analogous metabolite from BHT- d_{20} had lost one deuterium (m/z 268.2689), while BHT- d_3 lost its three labels (m/z 249.1504). Taken together, these results confirm this isomer as hydroxylated BHT-aldehyde (BHT-aldehyde + O).

DBP (2,6-di-tert-butylphenol) is a known metabolite of BHT. It is also used as a synthetic phenolic antioxidant in plastics and food packaging [30]. DBP was detected in oxidative incubations at 14.2 min with m/z 205.1600 (Table 1 and Figure 2). This metabolite has been confirmed by the synthetic DBP standard, which was also incubated under oxidative conditions (Figure S1). Further oxidation of DBP can form BHT-hydroquinone (BHQ), which was also detected in BHT incubations at 8.3 min (Table 1 and Figure 2). The loss of all three deuterium labels from BHT- d_3 and none from BHT- d_{20} confirm the *para*-hydroquinone structure (Table 2) of BHQ.

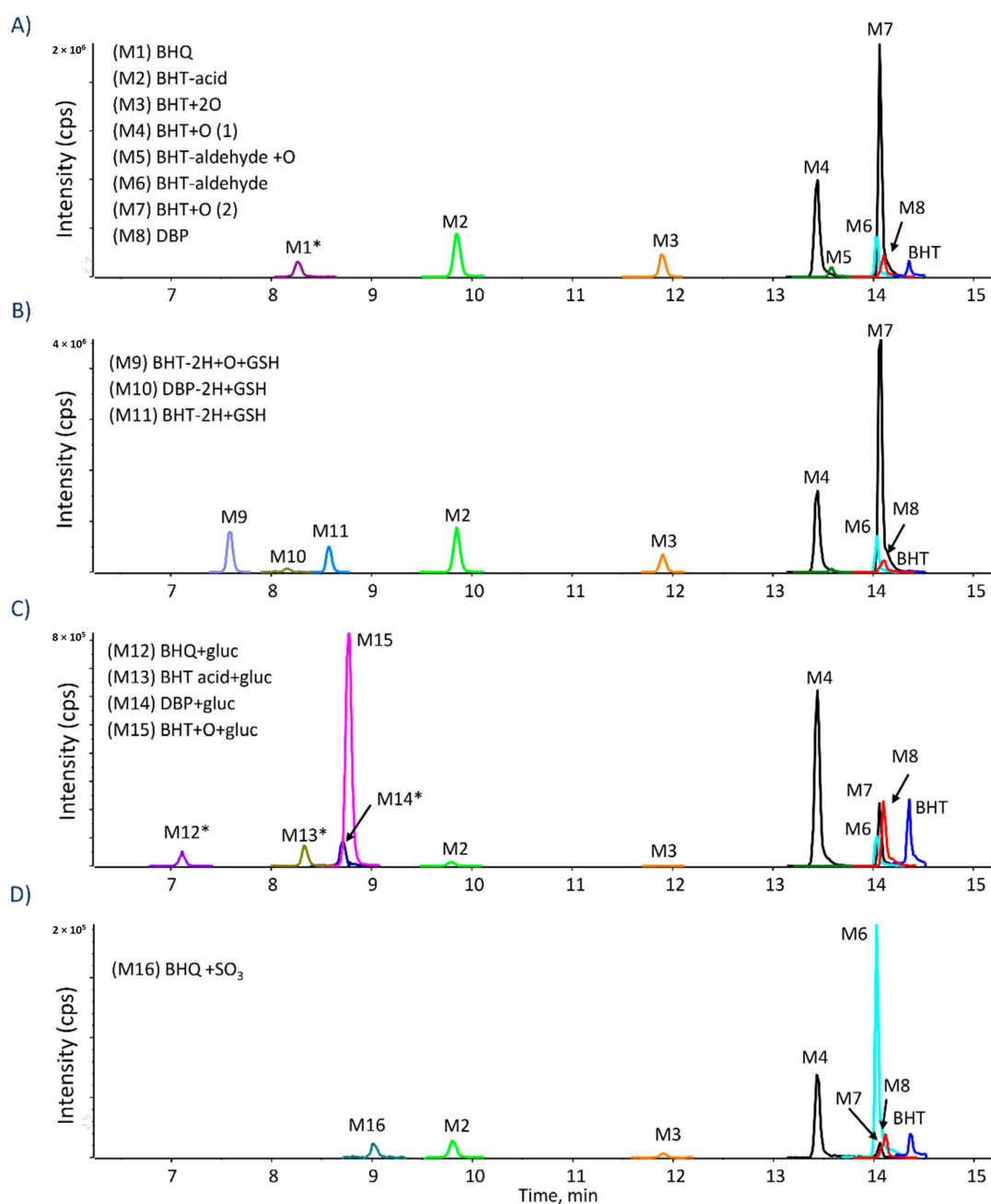


Figure 2. Extracted ion chromatograms of BHT metabolites formed in (A) HLM with NADPH; (B) HLM with NADPH and GSH; (C) HLM with NADPH and UDPGA; (D) Human S9 fraction with NADPH and PAPS; Peaks with asterisk. * were increased by 10×.

Numerous metabolites of BHT have been described and metabolic pathways proposed [6,31]. A major metabolic pathway is initiated by the oxidation of the *p*-methyl group, leading to the formation BHT-aldehyde and BHT-acid by stepwise oxidation. The acidic form is decarboxylated to DBP, from which BHQ is likely formed. Another metabolic pathway is initiated by the oxidation of the *t*-butyl group. The double oxidation forms BHT + 2O, being further oxidized into hydroxylated BHT-aldehyde (BHT-aldehyde + O) (Figure 3). Thompson et al. [32] studied the oxidative metabolism of BHT by hepatic and pulmonary rodent microsomes and identified several of these metabolites by LC-UV, GC-MS and using radiolabeled BHT (¹⁴C-BHT). The oxidative pathways of BHT have also been studied in vivo in different species, including the oxidation of the *p*-methyl group as a major metabolic route in rat, rabbit, and monkey, while the oxidation of *t*-butyl groups has been described

as the predominant pathway in human and mouse [33]. Zhang et al. [29] reported that BHT and its metabolites, including BHT-acid, BHQ, and BHT-aldehyde were present in metabolism-related organs (e.g., liver and kidney) in mouse.

Table 2. High-resolution mass spectrometry data using isotope-labeled BHT analogs.

Metabolite	BHT-d ₃ Formula <i>m/z</i> (ppm)	BHT-d ₂₀ Formula <i>m/z</i> (ppm)	Comments
BHT + O (1)	C ₁₅ D ₂ H ₂₂ O ₂ 237.1834 (2.1)	C ₁₅ D ₂₀ H ₄ O ₂ 255.2967 (3.2)	O added on <i>p</i> -CH ₃
BHT + O (2)	C ₁₅ D ₃ H ₂₁ O ₂ 238.1893 (0.7)	C ₁₅ D ₁₉ H ₄ O ₂ 254.2903 (2.6)	O added on <i>t</i> -butyl
BHT + 2O	C ₁₅ D ₂ H ₂₂ O ₃ 238.1893 (0.7)	C ₁₅ D ₁₉ H ₄ O ₃ 270.2855 (3.6)	O added on <i>p</i> -CH ₃ and <i>t</i> -butyl
BHT-aldehyde	C ₁₅ H ₂₂ O ₂ 233.1553 (2.5)	C ₁₅ D ₂₀ H ₂ O ₂ 253.2811 (3.4)	Aldehyde in <i>para</i> position
BHT-acid	C ₁₅ H ₂₂ O ₃ 249.1505 (3.5)	C ₁₅ D ₂₀ H ₂ O ₃ 269.2757 (2)	Carboxylic acid in <i>para</i> position
BHT-aldehyde + O	C ₁₅ H ₂₂ O ₃ 249.1504 (3.1)	C ₁₅ D ₁₉ H ₂ O ₃ 268.2689 (0.1)	CHO on <i>p</i> -methyl, OH on <i>t</i> -butyl
DBP	C ₁₄ H ₂₂ O 205.1607 (4.4)	C ₁₄ D ₂₀ H ₂ O 225.2861 (3.4)	DBP structure
BHQ	C ₁₄ H ₂₂ O ₂ 221.1548 (0.4)	C ₁₄ D ₂₀ H ₂ O ₂ 241.2797 (-2.2)	O added to DBP in <i>para</i> position
BHT-2H + GSH	C ₂₅ D ₂ H ₃₇ N ₃ O ₇ S 526.2560 (-0.2)	C ₂₅ D ₂₀ H ₁₉ N ₃ O ₇ S 544.3691 (-0.1)	SG group added to <i>p</i> -CH ₃
BHT + O-2H + GSH	C ₂₅ D ₂ H ₃₇ N ₃ O ₈ S 542.2508 (-0.4)	C ₂₅ D ₁₉ H ₂₀ N ₃ O ₈ S 559.3588 (1.8)	SG added to <i>p</i> -CH ₃ and O on <i>t</i> -butyl
DBP-2H + GSH	C ₂₄ H ₃₇ N ₃ O ₇ S 510.2274 (-1.1)	C ₂₄ D ₂₀ H ₁₇ N ₃ O ₇ S 530.3541 (1.2)	SG added to ring in <i>para</i> position
DBP + gluc	C ₂₀ H ₃₀ O ₇ 381.1924 (1.4)	C ₂₀ D ₂₀ H ₁₀ O ₇ 401.3184 (2.5)	Glucuronide on hydroxyl of DBP
BHT + O + gluc	C ₂₁ D ₃ H ₂₉ O ₈ 414.2222 (2.2)	C ₂₁ D ₁₉ H ₁₃ O ₈ 430.3218 (0.2)	Glucuronide on O added on <i>t</i> -butyl
BHT-acid + gluc	C ₂₁ H ₃₀ O ₉ 425.1821 (0.9)	C ₂₁ D ₂₀ H ₁₀ O ₉ 445.3068 (-1.0)	Glucuronide on carboxylic acid
BHQ + gluc	C ₂₀ H ₃₀ O ₈ 397.1877 (2.3)	C ₂₀ D ₂₀ H ₁₀ O ₈ 417.3120 (0.8)	Glucuronide added to <i>para</i> -OH
BHQ + SO ₃	C ₁₄ H ₂₂ O ₅ S 301.1116 (0.5)	C ₁₄ D ₂₀ H ₁₀ O ₉ 321.2369 (-0.4)	SO ₃ attached to BHQ

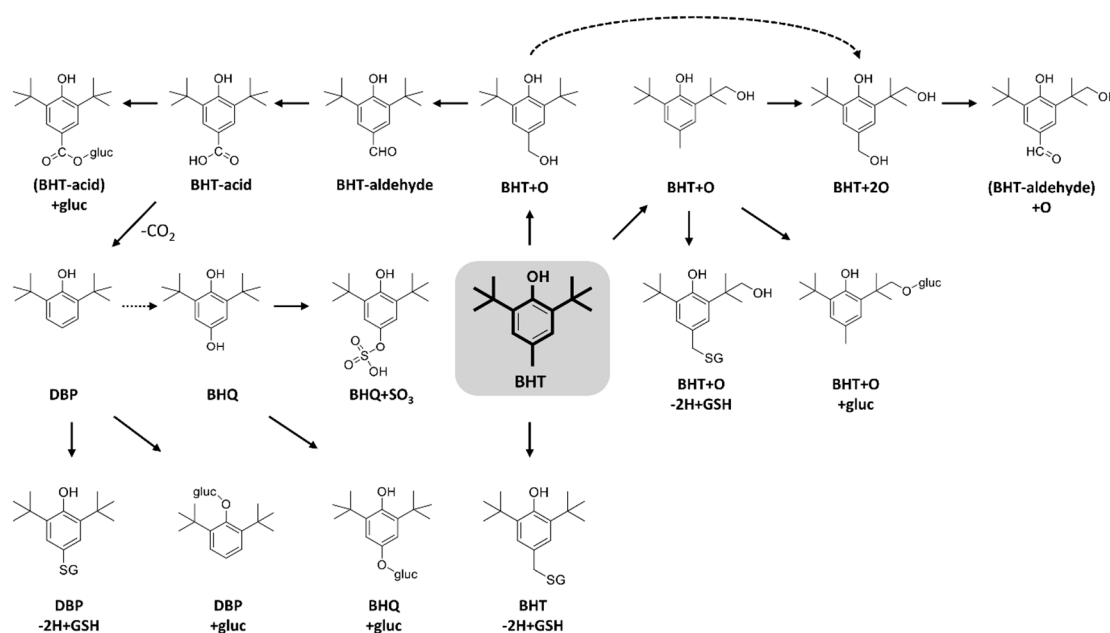


Figure 3. Proposed biotransformation reactions of BHT.

When GSH was added under oxidative conditions, three adducts were detected (Figure 2), corresponding to BHT-2H + GSH at 8.5 min, BHT + O-2H + GSH at 7.6 min, and DBP-2H + GSH at 8.2 min. HRMS/MS spectra for these adducts were dominated by characteristic peaks from the GSH moiety (m/z 306.077, 272.089, 254.078, 160.007, 143.046, and 128.035) (Table 1). The most prominent fragment ion for BHT-2H + GSH and BHT + O-2H + GSH was m/z 306.07 (Table 1), corresponding to deprotonated GSH. These two metabolites are proposed to result from the formation of the quinone methide intermediate followed by the addition of GSH on the methylene carbon. This hypothesis is supported by results from incubations with isotope-labeled BHT analogs. For BHT-2H + GSH, BHT- d_3 lost one deuterium, and none were lost from BHT- d_{20} . Tajima et al. [34] had also identified this metabolite by ^{13}C -NMR in rat bile. For BHT + O-2H + GSH, both BHT- d_3 and BHT- d_{20} lost one deuterium, confirming the same mechanism as above with the *t*-butyl being hydroxylated as well. This GSH adduct was also described by Madsen et al. where they compared electrochemical and enzymatic formation of several reactive metabolites [35].

The deprotonated ion of DBP-2H + GSH did not form m/z 306 upon CID and instead had a unique fragment ion at m/z 237.1316, assigned as deprotonated DBP with the sulfur of GSH still attached. The HR-MS spectra of isotope-labeled analogs showed the loss of the three labels from BHT- d_3 , while none were lost from BHT- d_{20} (Table 2). This supports the structure where the SG group replaces the methyl group. The formation of this metabolite is explained by a radical pathway, initiated by the decarboxylation of BHT-acid to form DBP \cdot , followed by GSH trapping. Glutathione is able to scavenge radicals by its electron-donating ability, enabling it to neutralize such reactive species. This GSH adduct had not been described in previous studies.

Several glucuronide conjugates were detected, including hydroxy-BHT glucuronide (BHT + O + gluc) at 8.8 min, BHT-acid glucuronide (BHT-acid + gluc) at 8.3 min, DBP glucuronide (DBP + gluc) at 8.7 min, and BHQ glucuronide (BHQ + gluc) at 7.1 min (Figure 2 and Table 1). The MS/MS spectra of these conjugates were dominated by characteristic peaks from the glucuronide moiety, at m/z 175, m/z 113, and m/z 85, as well as the neutral loss of $\text{C}_6\text{H}_8\text{O}_6$ (Table 1).

The only sulfate metabolite detected could be assigned as BHQ + SO_3 , eluting at 9.0 min (Figure 2). Its HRMS/MS spectra presented characteristic peaks of the sulfate conjugates at m/z 80.9645, m/z 79.9576 and m/z 221.1539 corresponding to the HSO_3^- ion, the sulfonate radical ion (SO_3^-), and the neutral loss of the SO_3 radical. This metabolite had not been reported previously.

2.2. Metabolism of BHA and TBHQ

BHA is an analog of BHT and has been used in different industries alone or in combination with BHT and other antioxidants. TBHQ is a metabolite of BHA through *O*-demethylation and a powerful synthetic phenolic antioxidant. BHA and TBHQ were also incubated under the same conditions studied for BHT. Table 3 summarizes LC-HRMS/MS results for BHA and all detected metabolites. The deprotonated molecules $[\text{M}-\text{H}]^-$ of BHA and TBHQ were detected at m/z 179.1084 and m/z 165.0921, with retention times at 12.7 and 9.6 min, respectively. Their MS/MS spectra (Figure 1) yielded common product ions at m/z 149.060 and 108.021, assigned as $\text{C}_9\text{H}_9\text{O}_2^-$ and $\text{C}_6\text{H}_4\text{O}_2^-$, respectively.

Two hydroxylated BHA metabolites (BHA + O) were detected (Figure S2) at 11.4 and 11.8 min (Table 3). No significant differences were seen in their MS/MS spectra. These hydroxylated BHA isomers were attributed to the fact that BHA is a mixture of two isomers, 2-BHA (10%) and 3-BHA (90%). Armstrong et al. [36] were the first to identify 3-BHA + O by incubating pure 3-BHA (99.5%) with RLM under oxidative conditions, using ^1H -NMR. Hydroxylated TBHQ (TBHQ + O) were also detected (Figure S3) at 8.2 min.

A dimer of BHA ($\text{C}_{22}\text{H}_{30}\text{O}_4$) was detected at 14.4 min (Figure S2), with m/z 357.2076 (1.5 ppm). Armstrong et al. [36] also described a di-BHA metabolite [36]. BHA dimer was also found to form in rat intestine and by incubating BHA with rat intestine peroxidase, as well as horseradish peroxidase [37]. No dimer was detected for TBHQ under our conditions, which may be explained by its preference to form the quinone reactive metabolite.

Table 3. Summary of MS/MS data for BHA metabolites in negative ion mode.

Metabolite	Formula	m/z [M-H] ⁻	ppm	RT (min)	Selected MS/MS Fragments *
BHA	C ₁₁ H ₁₆ O ₂	179.1084	3.6	12.7	164.0838 , 149.0604 , 121.0656, 108.0213
BHA + O (1)	C ₁₁ H ₁₆ O ₃	195.1027	2.3	11.8	180.0795 , 165.0560 , 137.0609
BHA + O (2)	C ₁₁ H ₁₆ O ₃	195.1031	2.4	11.4	180.0784 , 165.0552
BHA dimer	C ₂₂ H ₃₀ O ₄	357.2076	1.5	14.4	342.1831 , 327.1608
BHA-2H + GSH	C ₂₁ H ₃₁ N ₃ O ₈ S	484.1760	0.2	5.8	272.0898 , 254.0791 , 211.0810 , 210.0884, 179.0456, 143.0461 , 128.0345
BHA + O-2H + GSH	C ₂₁ H ₃₁ N ₃ O ₉ S	500.1709	0.3	5.0	306.0759 , 272.0864, 254.0750, 210.0892, 179.0450, 160.0056, 143.0470, 128.0371
TBHQ-2H + GSH (1)	C ₂₀ H ₂₉ N ₃ O ₈ S	470.1602	-0.1	5.1	272.0924 , 254.0822 , 210.0916 , 197.0660 , 179.0479 , 146.0468, 143.0471 , 128.0358
TBHQ-2H + GSH (2)	C ₂₀ H ₂₉ N ₃ O ₈ S	470.1675	2.3	5.4	272.0925 , 254.0821 , 210.0911, 197.0662 , 185.0586, 179.0476, 166.0998, 146.0462, 143.0466 , 128.0358
TBHQ-4H + GSH	C ₂₀ H ₂₇ N ₃ O ₈ S	468.1446	0.6	6.4	339.1025, 272.0930 , 254.0811, 210.0896, 197.0657 , 195.0503 , 192.1049 , 179.0465, 146.0442, 143.0466 , 128.0353
TBHQ-4H + 2GSH	C ₃₀ H ₄₄ N ₆ O ₁₄ S ₂	775.2288	0.6	1.7	646.1861, 502.1334 , 468.1445, 306.0769, 272.0890, 254.0790, 229.0358, 195.0488, 143.0463
BHA + gluc	C ₁₇ H ₂₄ O ₈	355.1401	0.9	5.6	337.1300, 179.1082, 175.0252 , 164.0845 , 117.0196, 113.0243 , 85.0296, 75.0090, 59.0139
BHA + O + gluc (1)	C ₁₇ H ₂₄ O ₉	371.1351	1	5.7	353.1259, 265.1083, 195.1035 , 180.0800 , 175.0254, 113.0245, 85.0293, 75.0080, 59.0135
BHA + O + gluc (2)	C ₁₇ H ₂₄ O ₉	371.1357	2.6	6.6	195.1027 , 180.0792 , 175.0242, 113.0237, 85.0287
TBHQ + gluc	C ₁₆ H ₂₂ O ₈	341.1240	-0.4	3.4	175.0253, 165.0920 , 113.0247 , 85.0295, 59.0137
BHA + SO ₃ (1)	C ₁₁ H ₁₆ O ₅ S	259.0647	4.7	8.3	244.0405, 179.1070, 164.0842 , 149.0606, 70.9571
BHA + SO ₃ (2)	C ₁₁ H ₁₆ O ₅ S	259.0645	0.4	7.2	239.0718, 179.1077 , 164.0844 , 149.0635, 79.9571
BHA + O + SO ₃	C ₁₁ H ₁₆ O ₆ S	275.0597	0.8	8.4	195.1032 , 180.0794 , 165.0559, 79.9574
TBHQ + SO ₃	C ₁₀ H ₁₄ O ₅ S	245.0489	1.4	5.7	165.0923, 149.0607, 108.0213, 80.9651, 79.9572

* fragment ions of >20% intensity relative to base peak are listed here in bold, base peak in each spectrum in underlined.

Identical GSH adducts were detected for BHA and TBHQ, namely two isomers of TBHQ-2H + GSH (at 5.1 and 5.4 min), TBHQ-4H + GSH (at 6.4 min), and a di-glutathione adduct, TBHQ-4H + 2GSH (at 1.7 min) (Figures S2 and S3). The HRMS/MS spectra from these GSH adducts were dominated by characteristic fragment ions of deprotonated GSH (m/z 272, 254, 210, 179, 166, 143, and 128), with the exception of m/z 197.066 (C₁₀H₁₃O₂S⁻) for the two isomers, where the sulfur atom of GSH is still bound to deprotonated TBHQ (Table 3). These GSH adducts were also detected in rat bile and urine following TBHQ administration [38]. Peters et al. [38] reported three GSH conjugates of TBHQ in vivo, including 5-(GS)-TBHQ, 6-(GS)-TBHQ, and 3,6-(GS)₂-TBHQ by LC-MS and ¹H-NMR. They also

suggested that these conjugates could represent nephrotoxic metabolites, and may be responsible for the tumor-promoting effects of TBHQ and BHA [38]. Two novel BHA glutathione adducts have been detected here, namely BHA-2H + GSH (at 5.8 min) and BHA + O-2H + GSH (at 5.0 min) (Figure S2). The first is suggested to form via an epoxide followed by GSH addition and loss of a water molecule, while the second is likely formed via the *ortho*-quinone reactive metabolite.

Four BHA glucuronide conjugates were detected, namely TBHQ + gluc, BHA + gluc, and two isomers of BHA + O + gluc, at 3.4, 5.6, 5.7, and 6.6 min, respectively (Table 3). By comparing the MS/MS spectra of the two BHA + O + gluc isomers, the peak at 5.7 min showed a water loss at m/z 353.1259 ($C_{17}H_{20}O_7^-$, 2.1 ppm) proving that the oxygen is added to the *tert*-butyl group, and not in the ring as for the isomer detected at 6.6 min. These two novel metabolites have not been previously characterized. TBHQ also formed the same glucuronide conjugate as BHA (TBHQ + gluc) at 3.4 min (m/z 341.1240) with fragment ions mostly from the glucuronide moiety.

Several sulfate conjugates were detected for BHA, including two isomers corresponding to BHA + SO₃ at 7.2 and 8.3 min. Their MS/MS spectra yielded very similar fragments suggesting that one is 3-BHA + SO₃ and the other 2-BHA + SO₃ (Table 3). One peak corresponding to BHA + O + SO₃ was detected at 8.4 min. A common sulfate conjugate between BHA and TBHQ (TBHQ + SO₃) was also detected at 5.7 min. These same sulfate conjugates were previously detected in human urine using GC-MS [39]. The proposed biotransformation products of BHA and TBHQ are summarized in Figure 4.

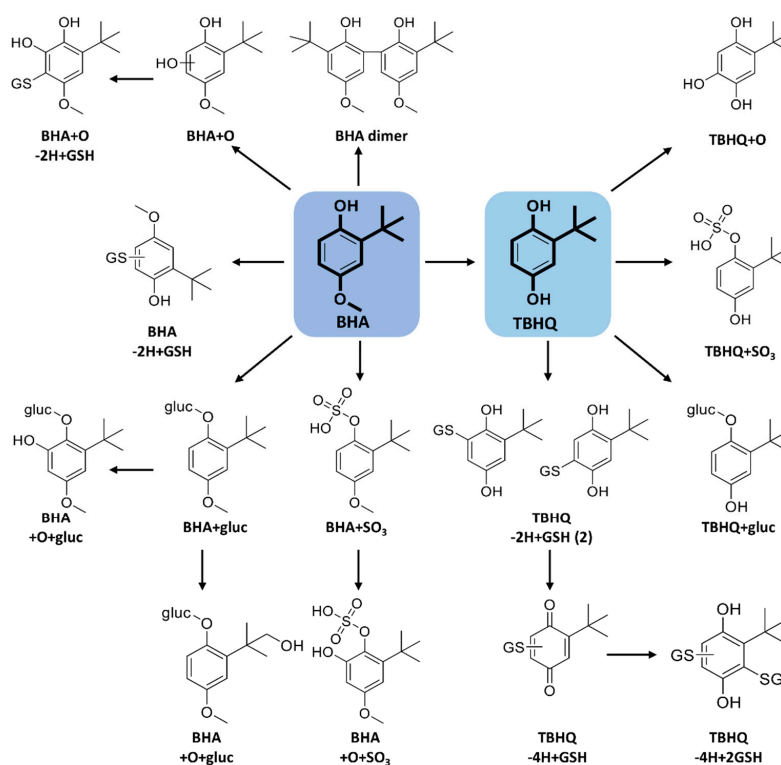


Figure 4. Proposed biotransformation reactions of BHA and TBHQ.

The major metabolic pathway for BHA is reported to be via the conjugation of the free hydroxyl group with both glucuronic acid and sulfate [39]. Conning et al. [33] reported that glucuronide conjugation predominates in rat, rabbit, and human, whereas sulfation is the major phase II reaction in dog. The major TBHQ metabolites found in rat bile and urine were TBHQ-glucuronide and TBHQ-sulfate [38].

2.3. Metabolism of DBP and BHT Acid

DBP and BHT acid standards were used to confirm these two metabolites of BHT, as mentioned above. The oxidative metabolism for these two compounds was also studied to help support the complex metabolic pathway proposed for BHT.

Under oxidative conditions, DBP formed previously uncharacterized oxidative metabolites, including a major metabolite hydroxylated of the *t*-butyl group (DBP + O), as well as two di-hydroxylated forms and a carboxylic acid metabolite (DBP + 2O–2H). Figure S1 shows the extracted ion chromatograms for DBP and BHT-acid oxidative metabolites, as well as a proposed scheme for their formation, supported by high-resolution MS/MS spectra for each metabolite.

The BHT-acid standard confirmed this BHT metabolite and helped distinguish it from the novel (BHT-aldehyde) + O. BHT-acid incubations showed that the formation of DBP and BHQ was non-enzymatic, and allowed a novel hydroxylated (BHT-acid + O) metabolite to be characterized (Figure S1).

By compiling the results from *in vitro* biotransformations of BHT, BHA, TBHQ, DBP, and BHT-acid, comprehensive schemes of the many metabolic transformations for these small synthetic antioxidants have been proposed. Using an untargeted high-resolution tandem mass spectrometry approach to decipher the metabolism of analogous compounds, while incorporating isotope labeling, proved to be a powerful method to elucidate structures of all detected metabolites.

3. Methods

3.1. Chemicals

Butylated hydroxytoluene [BHT, 2,6-di-*tert*-butyl-4-methylphenol,], butylated hydroxyanisole [BHA, 2(3)-*tert*-butyl-4-methoxyphenol (90%/10%)], *tert*-butylhydroquinone [TBHQ, 2-*tert*-butylbenzene-1,4-diol], 2,6-di-*tert*-butylphenol [DBP, 2,6-bis(*tert*-butyl)phenol], BHT acid [3,5-Di-*tert*-butyl-4-hydroxybenzoic acid], glutathione (GSH), uridine 5'-diphosphoglucuronic acid (UDPGA), 3'-phosphoadenosine-5'-phosphosulfate (PAPS), nicotinamide adenine dinucleotide phosphate (NADP⁺), glucose-6-phosphate, MgCl₂ and glucose-6-phosphate dehydrogenase, as well as HPLC-grade acetonitrile (ACN), methanol and formic acid were all purchased from Sigma-Aldrich (Oakville, ON, Canada). BHT-d₃ [2,6-di-*tert*-butyl-4-methyl-d₃-phenol] and BHT-d₂₁ [2,6-di-(*tert*-butyl-d₉)-4-methylphenol-3,5-d₂,OD] were purchased from CDN Isotopes (Pointe-Claire, QC, Canada). BHT-d₂₀ was created by heating the BHT-d₂₁ for 2 h at 60 °C. Human and rat liver microsomes (HLM and RLM) and human and rat liver S9 (HS9 and RS9) fractions were purchased from Corning (Corning, NY, USA). Ultrapure water was from a Millipore Synergy UV system (Billerica, MA, USA).

3.2. *In Vitro* Incubations

3.2.1. Oxidative Metabolites and GSH Adducts

BHT and analogs were incubated at 20 μM with human and rat liver microsomes (1 mg/mL protein) containing 5 mM GSH and a NADPH-regenerating system (5 mM MgCl₂, 0.5 mM NADP⁺, 10 mM glucose-6-phosphate and 2 units/mL glucose-6-phosphate dehydrogenase) at 37 °C for 1 h in 100 mM phosphate buffer, pH 7.4. Control samples were prepared without NADPH regenerating system and/or without GSH. Adding an equal volume of cold acetonitrile quenched the reaction. Incubation mixtures were centrifuged for 8 min at 14,000 rpm, at 4 °C. The supernatants were diluted (1:1) in water prior to LC-MS/MS analysis.

3.2.2. Phase II Metabolism—Glucuronidation and Sulfation

To study the glucuronide conjugates, all compounds (20 μM) were incubated with HLM and RLM (1 mg/mL protein), NADPH-regenerating system (as above), and 5 mM UDPGA at 37 °C for 1h. Each compound (20 μM) was also incubated with human and rat S9 fractions (2 mg/mL) in phosphate buffer, containing 1 mM of PAPS with the NADPH-regenerating system, to study the formation of

sulfates conjugates. All samples were incubated at 37 °C for 1h, quenched, and centrifuged as above. Supernatants were diluted as above and subjected to LC-MS/MS analysis.

3.3. LC-HRMS/MS Analysis and Data Processing

LC-MS/MS analyses were performed using a Shimadzu Nexera HPLC coupled to a Sciex 5600 TripleTOF[®] (quadrupole-time-of-flight) system (Concord, ON, Canada), in negative electrospray mode.

Chromatographic separation was performed using a Phenomenex Kinetex biphenyl (100 × 2.1 mm, 2.6 µm) column, using mobile phases of 5 mM ammonium acetate in water and 100% ACN, at 0.25 mL/min and a column temperature of 40 °C. The injection volume was 25 µL. The HPLC gradient was as follows: 5% B held for 0.5 min, linearly increased to 30% at 8 min, up to 50% at 12 min, and 90% at 13 min, held for an additional 2 min.

Ion source parameters were as follows: ionization voltage at 5000 V, curtain gas of 35 psi, drying and nebulizer gases each at 50 psi, source temperature of 450 °C, and declustering potential of 60 V. TOF-MS spectra were acquired (with 250 ms accumulation time), followed by MS/MS in information-dependent acquisition (IDA) mode on the 5 most intense ions using dynamic background subtraction (175 ms each). Nitrogen was used as collision gas and collision energy was 30 ± 10 V. Metabolites that did not have high-quality MS/MS in IDA mode, targeted MS/MS mode was used in a second injection.

MetabolitePilot 2.0 (Sciex) software was employed to screen samples for potential metabolites using a set of known biotransformations, including oxidative reactions, GSH, glucuronide, and sulfate conjugates. PeakView 2.2 and MasterView 1.1 (Sciex) were also used for processing LC-MS/MS data to confirm and expand the list of features based on mass accuracy, isotope pattern, and MS/MS analysis.

4. Conclusions

The metabolism of BHT and several analogs were investigated *in vitro* using human and rat liver microsomes and S9 fractions. Many oxidative metabolites, GSH adducts, glucuronide, and sulfate conjugates were detected with excellent mass accuracy, some of which had not been previously reported. Structures of biotransformation products were elucidated by HRMS/MS data and supported using isotope-labeled analogs. These results have enabled many biotransformation products to be determined, which are potentially involved in the toxicity of these compounds. Knowledge of all these possible metabolites would be useful in assessing environmental exposure to these compounds.

Supplementary Materials: The following are available online at <http://www.mdpi.com/1422-0067/21/24/9525/s1>, Figure S1: Extracted ion chromatograms of oxidative metabolites formed when BHT-acid (A) and DBP (B) were incubated with HLM and NADPH. (C) Proposed biotransformation reactions of DBP and BHT-acid; Figure S2: Extracted ion chromatograms of BHA metabolites formed in HLM with added (A) NADPH, (B) NADPH and GSH, (C) NADPH and UDPGA, and (D) human S9 fraction with NADPH and PAPS. Figure S3: Extracted ion chromatograms of TBHQ metabolites formed in (A) HLM with NADPH; (B) HLM with NADPH and GSH; (C) HLM with NADPH and UDPGA; (D) human S9 fraction with NADPH and PAPS.

Author Contributions: O.O. did experimentation and wrote the first draft of the manuscript. L.S. conceived of and supervised the project and revised the manuscript. All authors have read and agreed to the published version of the manuscript.

Funding: This work was funded by the Natural Sciences and Engineering Research Council of Canada (NSERC, Discovery grant no. RGPIN 2016-06034).

Acknowledgments: We acknowledge support of our mass spectrometry platform from the CERMO-FC (Centre d'excellence de recherche sur les maladies orphelines—Fondation Courtois). L.S. holds an institutional strategic chair from UQAM in bioanalytical chemistry.

Conflicts of Interest: The authors declare no conflict of interest.

References

1. Nieva-Echevarría, B.; Manzanos, M.J.; Goicoechea, E.; Guillén, M.D. 2, 6-Di-tert-butyl-hydroxytoluene and its metabolites in foods. *Compr. Rev. Food Sci.* **2015**, *14*, 67–80. [[CrossRef](#)]
2. Tortosa, V.; Pietropaolo, V.; Brandi, V.; Macari, G.; Pasquadibisceglie, A.; Polticelli, F. Computational Methods for the Identification of Molecular Targets of Toxic Food Additives. Butylated Hydroxytoluene as a Case Study. *Molecules* **2020**, *25*, 2229. [[CrossRef](#)] [[PubMed](#)]
3. Liu, R.; Mabury, S.A. Synthetic Phenolic Antioxidants in Personal Care Products in Toronto, Canada: Occurrence, Human Exposure, and Discharge via Greywater. *Environ. Sci. Technol.* **2019**, *53*, 13440–13448. [[CrossRef](#)] [[PubMed](#)]
4. Saad, B.; Sing, Y.Y.; Nawwi, M.A.; Hashim, N.; Ali, A.S.M.; Saleh, M.I.; Sulaiman, S.F.; Talib, K.M.; Ahmad, K. Determination of synthetic phenolic antioxidants in food items using reversed-phase HPLC. *Food Chem.* **2007**, *105*, 389–394. [[CrossRef](#)]
5. Liu, R.; Mabury, S.A. Synthetic phenolic antioxidants and transformation products in human sera from United States donors. *Environ. Sci. Technol. Lett.* **2018**, *5*, 419–423. [[CrossRef](#)]
6. Lanigan, R.S.; Yamarik, T.A. Final report on the safety assessment of BHT(1). *Int. J. Toxicol.* **2002**, *21* (Suppl. 2), 19–94.
7. Ahmad, H.; Sharma, R.; Mansour, A.; Awasthi, Y.C. t-butylated hydroxytoluene enhances intracellular levels of glutathione and related enzymes of rat lens in vitro organ culture. *Exp. Eye Res.* **1992**, *54*, 41–48. [[CrossRef](#)]
8. Botterweck, A.A.; Verhagen, H.; Goldbohm, R.A.; Kleinjans, J.; van den Brandt, P.A. Intake of butylated hydroxyanisole and butylated hydroxytoluene and stomach cancer risk: Results from analyses in the Netherlands Cohort Study. *Food Chem. Toxicol.* **2000**, *38*, 599–605. [[CrossRef](#)]
9. Nagai, F.; Ushiyama, K.; Kano, I. DNA cleavage by metabolites of butylated hydroxytoluene. *Arch. Toxicol.* **1993**, *67*, 552–557. [[CrossRef](#)]
10. Kupfer, R.; Dwyer-Nield, L.D.; Malkinson, A.M.; Thompson, J.A. Lung toxicity and tumor promotion by hydroxylated derivatives of 2,6-di-tert-butyl-4-methylphenol (BHT) and 2-tert-butyl-4-methyl-6-iso-propylphenol: Correlation with quinone methide reactivity. *Chem. Res. Toxicol.* **2002**, *15*, 1106–1112. [[CrossRef](#)]
11. Sun, Z.; Yang, X.; Liu, Q.S.; Li, C.; Zhou, Q.; Fiedler, H.; Liao, C.; Zhang, J.; Jiang, G. Butylated hydroxyanisole isomers induce distinct adipogenesis in 3T3-L1 cells. *J. Hazard Mater.* **2019**, *379*, 120794. [[CrossRef](#)] [[PubMed](#)]
12. Goodman, D.L.; McDonnell, J.T.; Nelson, H.S.; Vaughan, T.R.; Weber, R.W. Chronic urticaria exacerbated by the antioxidant food preservatives, butylated hydroxyanisole (BHA) and butylated hydroxytoluene (BHT). *J. Allergy Clin. Immunol.* **1990**, *86*, 570–575. [[CrossRef](#)]
13. World Health Organization (WHO); International Agency for Research on Cancer (IARC). Some naturally occurring and synthetic food components, furocoumarins and ultraviolet radiation, Summary of Data Reported and Evaluation. In *IARC Monographs on the Evaluation of Carcinogenic Risks to Humans*; IARC: Lyon, France, 1986; Volume 40, pp. 123–206.
14. Ansar, S.; Iqbal, M. Antioxidant and nephroprotective potential of butylated hydroxyanisole against ferric nitrilotriacetate-induced oxidative stress and early tumor events. *Hum. Exp. Toxicol.* **2016**, *35*, 448–453. [[CrossRef](#)] [[PubMed](#)]
15. Singh, B.; Mense, S.M.; Remotti, F.; Liu, X.; Bhat, H.K. Antioxidant butylated hydroxyanisole inhibits estrogen-induced breast carcinogenesis in female ACI rats. *J. Biochem. Mol. Toxicol.* **2009**, *23*, 202–211. [[CrossRef](#)] [[PubMed](#)]
16. Ito, N.; Fukushima, S.; Tsuda, H. Carcinogenicity and modification of the carcinogenic response by BHA, BHT, and other antioxidants. *Crit. Rev. Toxicol.* **1985**, *15*, 109–150. [[CrossRef](#)] [[PubMed](#)]
17. Pop, A.; Kiss, B.; Loghin, F. Endocrine disrupting effects of butylated hydroxyanisole (BHA-E320). *Clujul Med.* **2013**, *86*, 16–20.
18. Choe, S.; Yang, K. Toxicological studies of antioxidants, butylated hydroxytoluene (BHT) and butylated hydroxyanisole (BHA). *Korean J. Food Nutr.* **1982**, *14*, 283–288.
19. Gharavi, N.; Haggarty, S.; El-Kadi, A.O. Chemoprotective and carcinogenic effects of tert-butylhydroquinone and its metabolites. *Curr. Drug Metab.* **2007**, *8*, 1–7. [[CrossRef](#)]
20. Almeida, E.S.; Portela, F.M.; Sousa, R.M.; Daniel, D.; Terrones, M.G.; Richter, E.M.; Muñoz, R.A. Behaviour of the antioxidant tert-butylhydroquinone on the storage stability and corrosive character of biodiesel. *Fuel* **2011**, *90*, 3480–3484. [[CrossRef](#)]

21. Van Esch, G.J. Toxicology of tert-butylhydroquinone (TBHQ). *Food Chem. Toxicol.* **1986**, *24*, 1063–1065. [CrossRef]
22. Li, C.; Cui, X.; Chen, Y.; Liao, C.; Ma, L.Q. Synthetic phenolic antioxidants and their major metabolites in human fingernail. *Environ. Res.* **2019**, *169*, 308–314. [CrossRef] [PubMed]
23. Zhang, R.; Li, C.; Li, Y.; Cui, X.; Ma, L.Q. Determination of 2,6-di-tert-butyl-hydroxytoluene and its transformation products in indoor dust and sediment by gas chromatography-mass spectrometry coupled with precolumn derivatization. *Sci. Total Environ.* **2018**, *619–620*, 552–558. [CrossRef] [PubMed]
24. Wang, W.; Kannan, K. Quantitative identification of and exposure to synthetic phenolic antioxidants, including butylated hydroxytoluene, in urine. *Environ. Int.* **2019**, *128*, 24–29. [CrossRef]
25. E 320 Butylated Hydroxy-Anisole (BHA). The UK Food Guide. Available online: <http://ukfoodguide.net/e321.htm> (accessed on 25 October 2020).
26. Health Canada. 2020. List of Permitted Preservatives. Available online: <https://www.canada.ca/en/health-canada/services/food-nutrition/food-safety/food-additives/lists-permitted/11-preservatives.html#a4> (accessed on 30 August 2020).
27. Suh, H.J.; Chung, M.S.; Cho, Y.H.; Kim, J.W.; Kim, D.H.; Han, K.W.; Kim, C.J. Estimated daily intakes of butylated hydroxyanisole (BHA), butylated hydroxytoluene (BHT) and tert-butyl hydroquinone (TBHQ) antioxidants in Korea. *Food Addit. Contam.* **2005**, *22*, 1176–1188. [CrossRef] [PubMed]
28. Fries, E.; Puttmann, W. Analysis of the antioxidant butylated hydroxytoluene (BHT) in water by means of solid phase extraction combined with GC/MS. *Water Res.* **2002**, *36*, 2319–2327. [CrossRef]
29. Zhang, R.; Li, J.; Cui, X. Tissue distribution, excretion, and metabolism of 2, 6-di-tert-butyl-hydroxytoluene in mice. *Sci. Total Environ.* **2020**, *739*, 139862. [CrossRef] [PubMed]
30. Yang, Y.; Hu, C.; Zhong, H.; Chen, X.; Chen, R.; Yam, K.L. Effects of Ultraviolet (UV) on Degradation of Irgafos 168 and Migration of Its Degradation Products from Polypropylene Films. *J. Agric. Food Chem.* **2016**, *64*, 7866–7873. [CrossRef]
31. Pont, M.M. *Health-Based Reassessment of Administrative Occupational Exposure Limits: 2, 6-Di-tert-butyl-p-cresol (BHT/Butylated Hydroxytoluene)*; Gezondheidsraad: The Hague, The Netherlands, 2004.
32. Thompson, J.A.; Malkinson, A.M.; Wand, M.D.; Mastovich, S.L.; Mead, E.W.; Schullek, K.M.; Laudenschlager, W.G. Oxidative metabolism of butylated hydroxytoluene by hepatic and pulmonary microsomes from rats and mice. *Drug Metab. Dispos.* **1987**, *15*, 833–840.
33. Conning, D.M.; Phillips, J.C. Comparative metabolism of BHA, BHT and other phenolic antioxidants and its toxicological relevance. *Food Chem. Toxicol.* **1986**, *24*, 1145–1148. [CrossRef]
34. Tajima, K.; Yamamoto, K.; Mizutani, T. Identification and determination of glutathione and glucuronide conjugates formed from butylated hydroxytoluene in rats. *Chem. Pharm. Bull.* **1983**, *31*, 3671–3677. [CrossRef]
35. Madsen, K.G.; Olsen, J.; Skonberg, C.; Hansen, S.H.; Jurva, U. Development and evaluation of an electrochemical method for studying reactive phase-I metabolites: Correlation to in vitro drug metabolism. *Chem. Res. Toxicol.* **2007**, *20*, 821–831. [CrossRef] [PubMed]
36. Armstrong, K.E.; Wattenberg, L.W. Metabolism of 3-tert-butyl-4-hydroxyanisole to 3-tert-butyl-4,5-dihydroxyanisole by rat liver microsomes. *Cancer Res.* **1985**, *45*, 1507–1510. [PubMed]
37. Sgaragli, G.; Corte, L.D.; Puliti, R.; De Sarlo, F.; Francalanci, R.; Guarna, A.; Dolara, P.; Komarynsky, M. Oxidation of 2-t-butyl-4-methoxyphenol (BHA) by horseradish and mammalian peroxidase systems. *Biochem. Pharmacol.* **1980**, *29*, 763–769. [CrossRef]
38. Peters, M.M.; Lau, S.S.; Dulik, D.; Murphy, D.; van Ommen, B.; van Bladeren, P.J.; Monks, T.J. Metabolism of tert-butylhydroquinone to S-substituted conjugates in the male Fischer 344 rat. *Chem. Res. Toxicol.* **1996**, *9*, 133–139. [CrossRef]
39. El-Rashidy, R.; Niazi, S. A new metabolite of butylated hydroxyanisole in man. *Biopharm. Drug Dispos.* **1983**, *4*, 389–396. [CrossRef]

Publisher's Note: MDPI stays neutral with regard to jurisdictional claims in published maps and institutional affiliations.



© 2020 by the authors. Licensee MDPI, Basel, Switzerland. This article is an open access article distributed under the terms and conditions of the Creative Commons Attribution (CC BY) license (<http://creativecommons.org/licenses/by/4.0/>).